SKB

TECHNICAL REPORT

89-38

An estimation of nuclide release rate near the canister (Near Field Model 91)

Han-Soo Lee[1], Luis Moreno[2], Ivars Neretnieks[2], Lennart Nilson[3]

[1] Dept. of Radwaste Disposal, Korea Advanced Energy Research Institute, Choong-Nam, Korea
[3] Dept. of Chemical Engineering, Royal Institute of Technology, Stockholm, Sweden

December 1989

SVENSK KÄRNBRÄNSLEHANTERING AB
SWEDISH NUCLEAR FUEL AND WASTE MANAGEMENT CO

BOX 5864 S-102 48 STOCKHOLM

TEL 08-665 28 00 TELEX 13108 SKB S
TELEFAX 08-661 57 19

AN ESTIMATION OF NUCLIDE RELEASE RATE NEAR THE CANISTER
(Near Field Model 91)

Han-Soo Lee[1], Luis Moreno[2], Ivars Neretnieks[2], Lennart Nilson[2]

1 Dept. of Radwaste Disposal, Korea Advanced Energy Research Institute, Choong-Nam, Korea

2 Dept. of Chemical Engineering, Royal Institute of Technology, Stockholm, Sweden

December 1989

Information on SKB technical reports from 1977-1978 (TR 121), 1979 (TR 79-28), 1980 (TR 80-26), 1981 (TR 81-17), 1982 (TR 82-28), 1983 (TR 83-77), 1984 (TR 85-01), 1985 (TR 85-20), 1986 (TR 86-31), 1987 (TR 87-33) and 1988 (TR 88-32) is available through SKB.

AN ESTIMATION OF NUCLIDE RELEASE RATE NEAR THE CANISTER
(Near Field Model 91)

Han-Soo Lee*, Luis Moreno+, Ivars Neretnieks+
and Lennart Nilson+

* Dept. of Radwaste Disposal
Korea Advanced Energy Research Institute
P.O.Box 7, Daeduk-Danji,Choong-Nam
Korea

\+ Dept. of Chemical Engineering
Royal Institute of Technology
100 44 Stockholm
Sweden

December 1989

ABSTRACT

Radionuclide release from the degraded canister to the mobile water in the rock has been modelled and several different pathways have been investigated. They include transport through the rock to the water by diffusion as well as directly into the mouth of the fractures via the backfill. The importance of the different paths and the various resistances to transport are discussed and numerical sample calculations are given.

TABLE OF CONTENTS

SUMMARY

The transport rates of radionuclides from a canister to the mobile water in fractures in the rock has been calculated for several pathways. They include the diffusion through the backfill via the rock and further into the mobile water in the fractures. Another pathway which leads directly from the backfill and into the mouth of the fracture has also been calculated and compared to the path via the rock. The influence of a possible sealing of the fracture on the transport rate has also been investigated.

The results show that the pathway through the rock conveys less nuclides than the pathway directly to the fracture mouth. Sealing the fracture for a few tens of cm considerably decreases the release.

1 INTRODUCTION AND BACKGROUND

In Sweden, the final repository for the storage of high level waste is to be located deep down in a bedrock of very low permeability. The high level waste contains long lived nuclides. If released they will migrate to the biosphere carried by the groundwater. In order to decrease the release rate of nuclides from the repository, the waste is enclosed in canisters. These canisters are placed in holes in the bedrock and the space between the canister and rock is filled with a backfill material of very low hydraulic conductivity which will decrease waterflow to the canister to very low values. Nuclides will move through the backfill mainly by diffusion (Neretnieks,1977).

Nuclides which escape from a penetrated or degraded canister will diffuse through the backfill to the rock and further through the rock until they enter some mobile water in a fracture. They will then be picked up by the water and swept away. Some fractures are bound to intersect the hole and if the fractures are open and have water flow in them this mobile water will be in direct contact with the buffer and nuclides may be picked up by this water without them having to diffuse through the rock first. It has been proposed that the fractures nearest the deposition hole be sealed with some stable material so that the mobile water will not be in direct contact with the backfill in the hole. One of the main aims of this report is to model the migration of the nuclides, to investigate the relative importance of the different pathways and to assess the impact of sealing.

A simple model for the analysis of two dimensional transport in the backfill and the uptake in the mobile water in the fracture was proposed by Neretnieks (1978). Andersson et al.(1982) used a numerical approach to model three dimensional diffusion of the nuclides in the backfill as well as the subsequent uptake in the water. A simpler model taking into account the 2 or 3 dimensional diffusion in the backfill material was developed and solved analytically assuming constant flux at the fracture aperture

(Neretnieks,1986). In all these models it was assumed that the nuclides do not penetrate into the porous rock.

The present study is aimed at modelling the transport of nuclides in the backfill as well as in the rock near the canister. Two different situations are modelled in order to compare the relative importance of the different nuclide paths. In the first case the nuclides migrate through the backfill and enter only the fracture aperture. The rock matrix is assumed to be impermeable. In the second case the fracture aperture is completely sealed so that nuclide must diffuse through the porous rock to reach the mobile water.

Both analytical and numerical methods are used in this study. The analytical methods are difficult to apply to some of the cases of interest but are very useful for studying the general properties of the solutions. Furthermore they are used to test the accuracy of the numerical methods and to lend credibility to the results.

2 THE STUDIED CASES: CONCEPTUAL MODELS

For modelling purposes the canister is assumed to be very long and the rock is assumed to be intersected by fractures at regular intervals. The region between two fractures can then be modelled utilizing the planes of symmetry. Figure 1 shows a section of a canister with a fracture intersecting it perpendicularly.

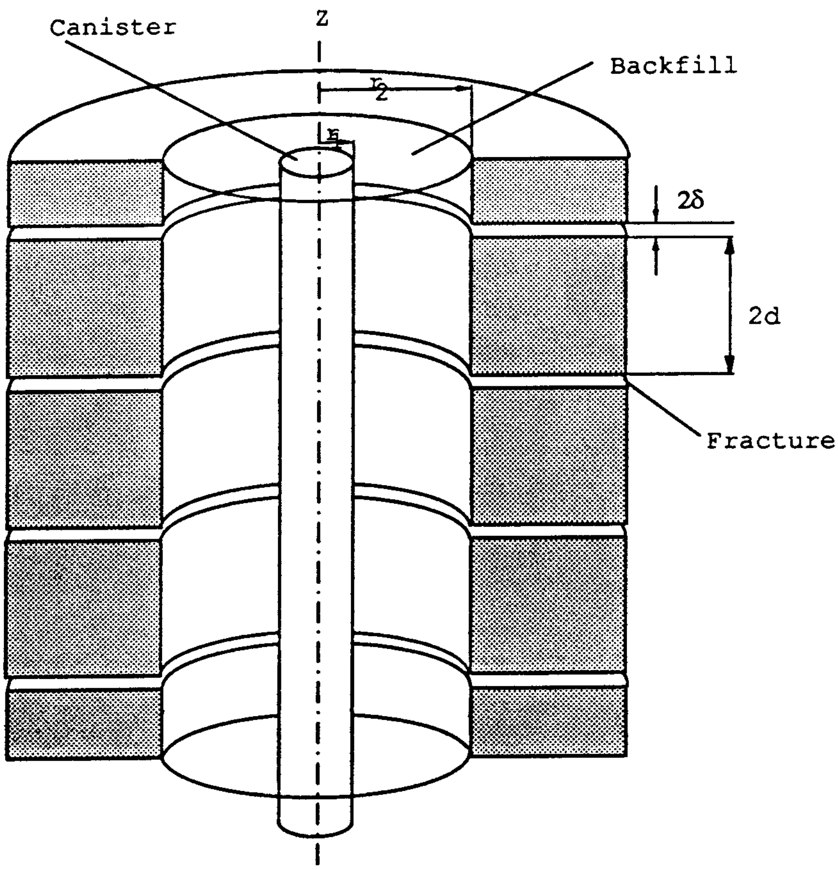

Figure 1 Fractures intersecting a repository hole with a canister.

To further simplify the modelling at this stage only a sector of the region around the canister is modelled as shown in figure 2. The geometry of the sector is further simplified by transformation to a parallellepiped, whereby rectangular symmetry is achieved. This considerably simplifies the analytical solutions without introducing

errors more than by a factor of about 2 for the the cases studied as can be found from the analytical solutions for both rectangular and cylindrical symmetry presented by Neretnieks (1986).

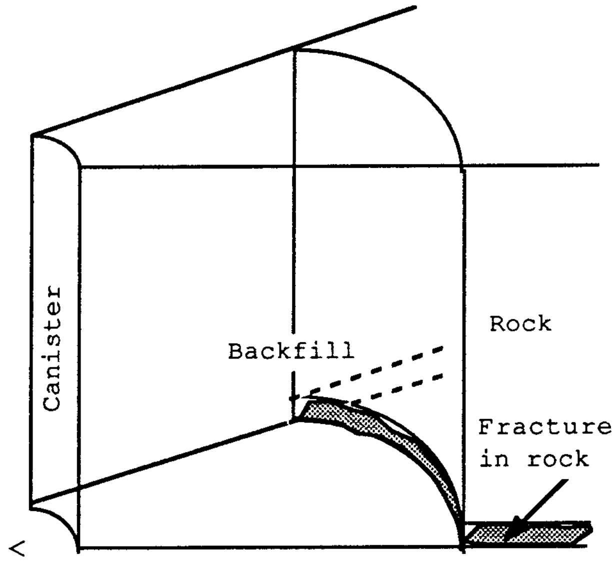

Figure 2 A sector of the backfill with the canister and the rock with the fracture.

In addition the following limitations and assumptions were made

1. The diffusivities of the backfill material and the porous rock were assumed to be constant but not the same.

2. Only the steady state transport of very long-lived nuclides is calculated.

3. The water flow is so high that the nuclide concentration in the fracture is zero.

4. The nuclide concentration at the wall of the canister is constant.

2.1 DIFFUSION INTO THE FRACTURE APERTURE - ROCK IMPERMEABLE TO DIFFUSION

When the rock is assumed to be impermeable, the nuclides diffuse only into the fracture aperture. This case is shown in figure 3. In this figure the nuclide concentration at the canister is constant. With the exception of the fracture aperture, the boundary region at the rock interface is impermeable.

By the aforementioned assumptions the governing equation for the nuclide concentration can be written as follows.

$$\frac{\partial^2 c}{\partial x^2} + \frac{\partial^2 c}{\partial y^2} = 0 \qquad \text{...(1)}$$

The boundary conditions at y=0 and y=d are obtained from the symmetry assumption and they state that there is no flux over these boundaries. All the nuclide transport must thus go via the mouth of the fracture to reach the mobile water.

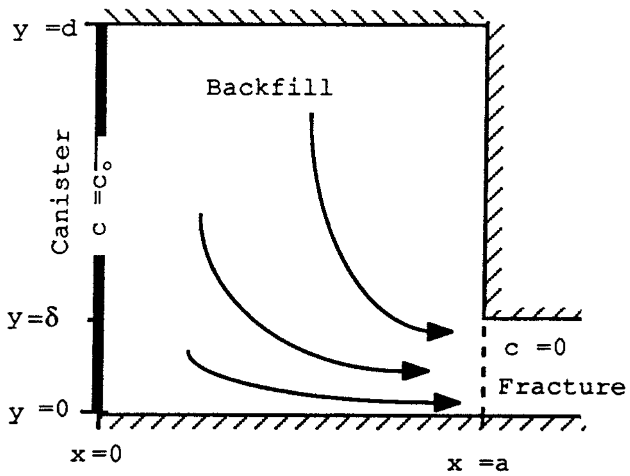

Figure 3 Schematic view of the region near the canister when the rock is assumed to be impermeable.

Thus

$$\left.\frac{\partial c}{\partial y}\right|_{y=0} = 0 \qquad \text{...(2)}$$

$$\left.\frac{\partial c}{\partial y}\right|_{y=d} = 0 \qquad \text{...(3)}$$

The concentration at the canister, x=0 is constant

$$c = c_0 \qquad (\text{ for } x=0) \qquad \ldots(4)$$

The boundary conditions at x=a are constant concentration at the fracture mouth and impermeable rock

$$c = 0 \qquad (0 < y < \delta) \qquad \ldots(5a)$$

and

$$\frac{\partial c}{\partial x}\Big|_{x=a} = 0 \qquad (\delta < y < d) \qquad \ldots(5b)$$

This case is not readily available for analytical treatment because of the mixed boundary conditions. A case which much resembles this case and where analytical solutions are available is used to study the properties around the narrow fracture mouth.

By stating that there is a constant flux across the fracture mouth, a certain location in the fracture mouth can be given the concentration zero. The concentration at other locations in the mouth can then be both less than and larger than zero. For a narrow aperture it is expected that the average flux for the two cases is nearly the same. Numerical calculations will be used to compare the solutions.

$$\frac{\partial c}{\partial x}\Big|_{x=a} = f(y) \qquad \ldots(6)$$

where f(y) = const for $0 < y < \delta$ and 0 for $\delta < y < d$.

For the boundary condition given in (6) the analytical solution was obtained while for the boundary condition according to (5a) and (5b) the numerical method was applied to get the solution.

It will be shown later that for a narrow fracture the solutions give very similar results.

2.2 DIFFUSION VIA THE ROCK - THE FRACTURE APERTURE IS PLUGGED.

The fracture aperture is assumed to be sealed completely and the nuclides diffuse through the porous rock to reach the fast flowing water (assumption to keep concentration equal to zero) in the fracture. The no flux boundary condition at the wall of the rock in the previous case, figure 3, is not valid. The impermeable boundary condition is instead applied for the fracture aperture. This is shown in figure 4.

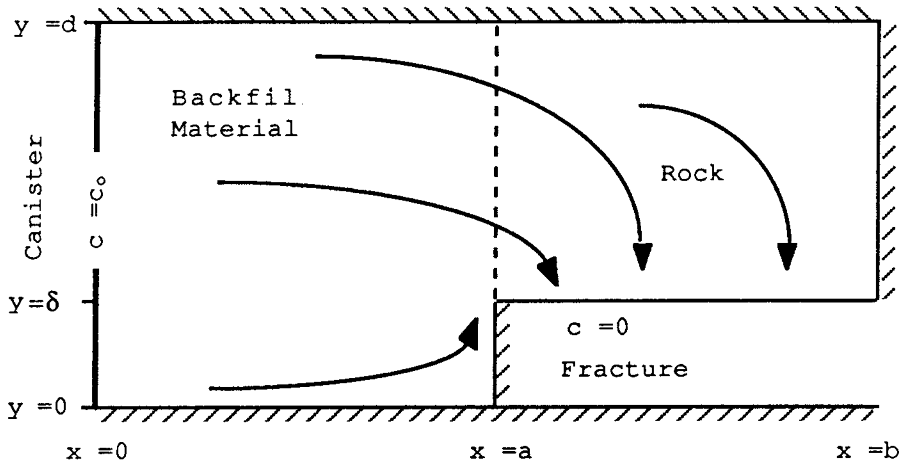

Figure 4 Schematic view near the canister when the fracture aperture is sealed.

The governing equation for the whole region is

$$\frac{\partial^2 c}{\partial x^2} + \frac{\partial^2 c}{\partial y^2} = 0 \qquad \ldots(7)$$

The boundary conditions are

$$\left.\frac{\partial c}{\partial y}\right|_{y=0} = 0 \qquad \text{for } 0 < x < a,\ y=0 \qquad \ldots(8)$$

$$c = 0 \qquad \text{for } a < x < b,\ y=\delta \qquad \ldots(9)$$

$$\left.\frac{\partial c}{\partial y}\right|_{y=d} = 0 \qquad \text{for } 0 < x < b,\ y=d \qquad \ldots(10)$$

$$c = c_0 \qquad \text{for } 0 < y < d,\ x=0 \qquad ...(11)$$

$$\frac{\partial c}{\partial x}\Big|_{x=a} = 0 \qquad \text{for } 0 < y < \delta,\ x=a \qquad ...(12)$$

$$\frac{\partial c}{\partial x}\Big|_{x=b} = 0 \qquad \text{for } \delta < y < d,\ x=b \qquad ...(13)$$

The continuity conditions at the interface, x=a are

$$D_1 \frac{\partial c_1}{\partial x} = D_2 \frac{\partial c_2}{\partial x} \qquad ...(14)$$

$$c_1 = c_2 \qquad ...(15)$$

where the subscripts 1 and 2 correspond to backfill material and rock respectively.

The governing equation (7) with the boundary conditions (8)-(15) was solved numerically by using the finite difference method as well as the integrated finite difference method (Lapidus and Pinder, 1982, Rasmusson et al, 1982).

2.3 DIFFUSION AROUND THE EDGE OF THE ROCK

In the problems studied here there are locations where a region with no flux is directly adjacent to a region with zero concentration and very high flux. Such points are very difficult to handle with numerical methods.It would be necessary to make very fine discretisations in the vicinity of such points to obtain good accuracy and it would still be difficult to know what errors would be obtained. Some analytical methods were therefore used to explore the properties of these regions.

For a case where the canister surface is directly in contact with the rock, due to the loss of the backfill material or a deformation of the hole, the concentration at

the rock surface becomes equal to the concentration at the canister surface (which was assumed to be equal to c_O). If the fracture aperture is sealed completely most of the mass flow goes just around the edge. This is shown in figure 5.

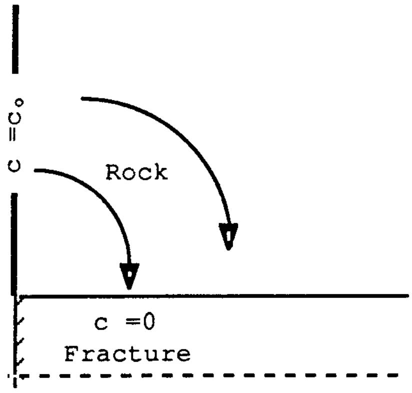

Figure 5 Schematic view near the edge of the rock.

Then the governing equation can be written in polar coordinates rather than in Cartesian coordinates.

$$\frac{\partial^2 c}{\partial r^2} + \frac{1}{r}\frac{\partial c}{\partial r} + \frac{1}{r^2}\frac{\partial^2 c}{\partial \theta^2} = 0 \qquad \text{...(16)}$$

$c(\theta = \pi/2) = c_O$ for all r ...(17)

$c(\theta = 0) = 0$ for all r ...(18)

$c(r = 0) =$ finite for $0 < \theta < \pi/2$ ...(19)

$c(r \to \infty) =$ finite for $0 < \theta < \pi/2$ ...(20)

The equation (16) with the boundary condition (17)-(20) can easily be solved (Carslaw and Jaeger, 1959).

3 RESULTS AND DISCUSSION

3.1 DIFFUSION INTO THE FRACTURE APERTURE

The analytical solution for equation (1) with the boundary conditions (2)-(4) and (6) is given as (Neretnieks, 1986)

$$\frac{c}{c_0} = 1 - \frac{N}{ADc_0}\left(\frac{\delta}{d}x + \sum_{n=1}^{\infty}\frac{2d}{(n\pi)^2}\cos\left(\frac{n\pi}{d}y\right)\sin\left(\frac{n\pi}{d}\delta\right)\frac{\sinh\left(\frac{n\pi}{d}x\right)}{\cosh\left(\frac{n\pi}{d}a\right)}\right) \quad \ldots(21a)$$

At a point in the fracture mouth with the coordinates x=a and y=δ/2, the concentration of the nuclides can be expressed as

$$\frac{c}{c_0} = 1 - \frac{N}{ADc_0}\left(\frac{\delta}{d}a + \sum_{n=1}^{\infty}\frac{2d}{(n\pi)^2}\cos\left(\frac{n\pi}{d}\frac{\delta}{2}\right)\sin\left(\frac{n\pi}{d}\delta\right)\frac{\sinh\left(\frac{n\pi}{d}a\right)}{\cosh\left(\frac{n\pi}{d}a\right)}\right) \quad \ldots(21b)$$

The summation of the series in equation (21) converges very slowly for small apertures (δ). The summation was made with a finite number of terms for a desired error bound. The term in the summation decreases with order of n^2. Thus the summation was terminated when the following term appears.

$$\frac{1}{n^2} < \varepsilon \quad \ldots(22)$$

When the value of δ is extremely small the absolute values of preceding terms are so small that those values are comparable with ε. In this case the summation is made over the first period of sinusoidal functions. The sum for the second period is then computed and compared with the first. If the sum over the second period is smaller than ε times the preceding sum, the calculation is terminated. Otherwise additional periods are calculated.

The concentration profile in the region is shown in figure 6. In this figure the most curved line corresponds to the concentration at x = a (fracture mouth). As shown in this figure the nearer the canister the location is, the

less change in concentration there is. Also the concentration along the system boundary at y=d remains practically constant irrespective of the position x.

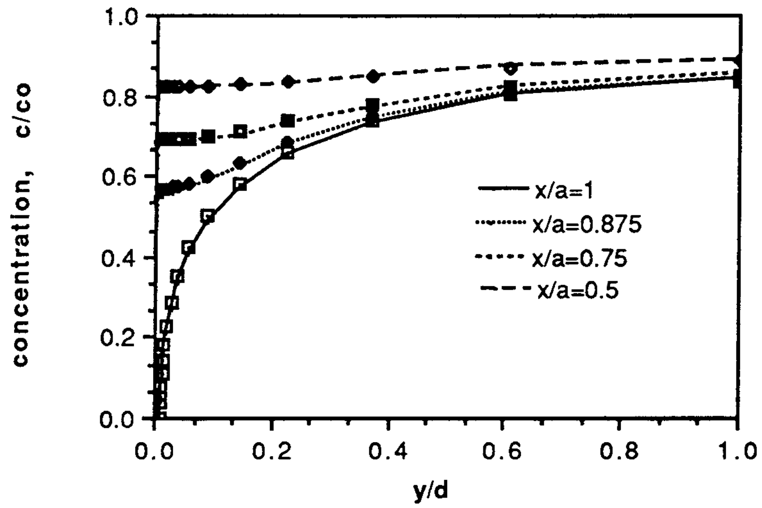

Figure 6 Comparison of analytical solution (lines) and numerical solution (marks) based on the same total flow rate for $\delta/d = 0.01$

Figure 6 also compares the analytical and numerical solutions. For our practical purposes thses solutions are equal and we can use the analytical solution which is based on constant flux to calculate the nuclide transport also for the case where the concentration is zero at the mouth of the fracture.

The analytical solution (21) gives the relation of the nuclide flow rate, N, with the fracture aperture. Let the summation term be F(x,y) then the nuclide flow rate can be expressed as

$$\frac{N}{DA(c_0-c)} = \frac{1}{F(x,y)} \qquad \text{...(23)}$$

where $A = 2\pi r_2 \delta$ is the surface area of the half of the fracture mouth within our system boundaries.

If both sides of equation (23) are multiplied by δ, the flow rate, expressed as the inverse of the equation (23),

i.e. as $F(x,y)/\delta$ can be represented as a function of δ/d, figure 7 (Neretnieks 1986). This figure shows that the mass flow rate decreases very slowly with decreasing fracture aperture.

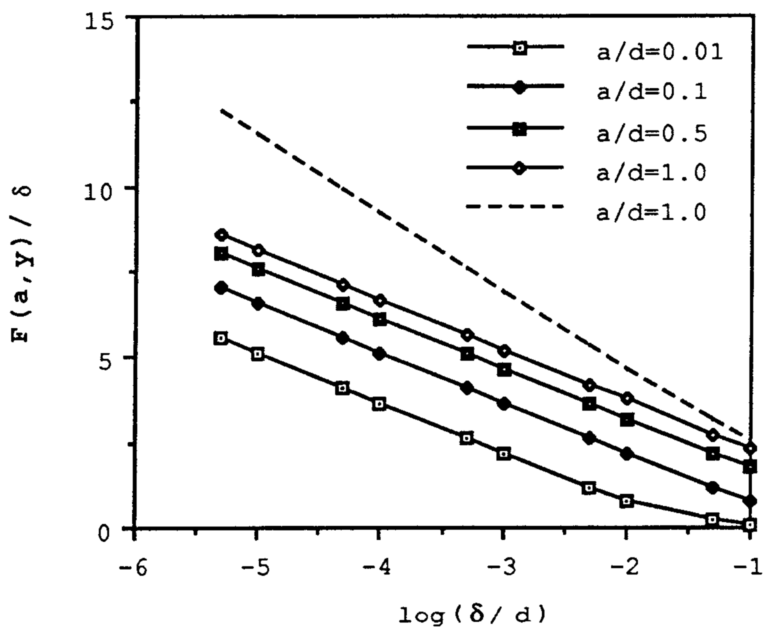

Figure 7 The function $F(a,y)/\delta$ versus $\log(\delta/d)$ with a/d as parameter (the dashed line is calculated by using a logarithmic approximation (Neretnieks, 1986))

Another way of describing the influence of the fracture aperture on the flow rate of nuclides into the fracture is to introduce a dimensionless flow rate, Γ, defined as the ratio $\frac{N}{N^0}$, where $N^0 = DA^0 \frac{\Delta c}{a}$, A^0 being the surface area of the hole. N^0 represents the flow rate that would occur when δ=d, corresponding to a case where there would be no resistance to the flow from the surrounding rock.

$\frac{N}{N^0}$ is obtained by multiplying both sides of equation (23) by the factor $\frac{\delta \cdot a}{d}$. $\Gamma = f(\frac{\delta}{d})$ is shown in figure 8.

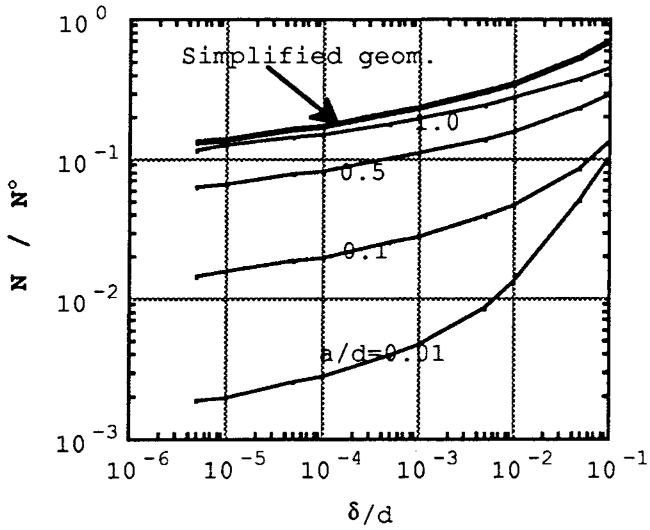

Figure 8 Dimensionless flow rate of nuclides, Γ, as function of δ/d. The concentration in the fracture is zero.

3.1.1 Zero concentration boundary condition

When the boundary condition of zero concentration is applied instead of the constant flux boundary condition the governing equation was solved numerically. In figure 6, the numerical solution was compared with the analytical solution. Even though different boundary conditions are applied the solutions are in good agreement when the flux is averaged over the whole fracture aperture.

The flux at the fracture aperture is shown in figure 9. This shows that the flux at the point of the boundary between the aperture and rock is larger than those for the other points, especially for small fracture apertures.

The influence of the fracture aperture on the equivalent mass flow rate, Qeq = N/c_0 is shown in figure 10.The effective diffusivity in the backfill is $4 \cdot 10^{-11}$ m^2/s, this is the same value as that used in KBS-3 (KBS-3, 1983).

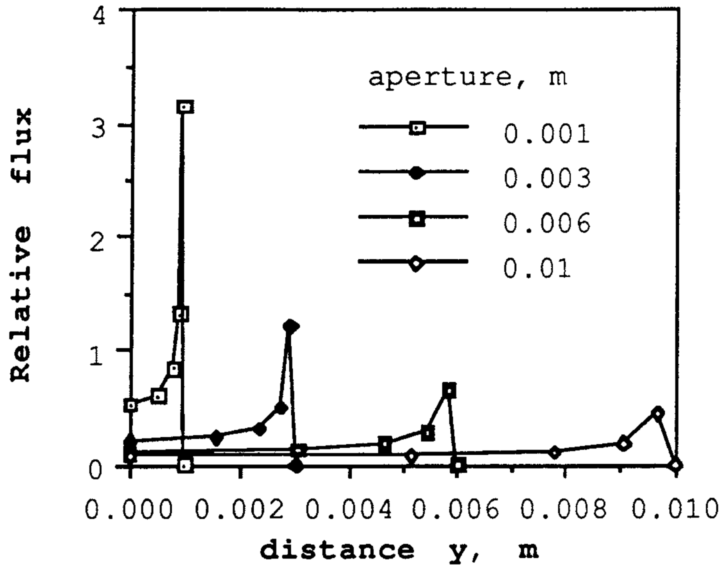

Figure 9 Flux across the fracture aperture when the concentration is zero.

Again it may be noted that the fracture aperture has a small influence on the nuclide flow rate. A three orders of magnitude change in aperture changes the nuclide flow rate by a factor of less than three.

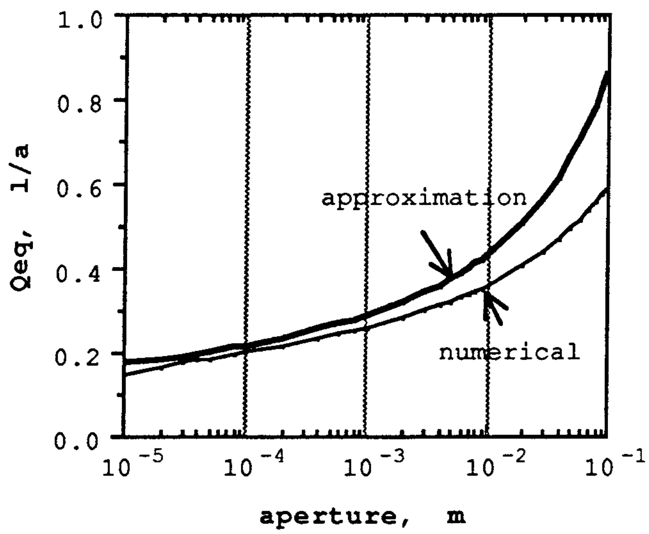

Figure 10 Equivalent flow rate, Q_{eq} dependency on the fracture aperture, for c=0 in the fracture.

3.1.2 Upper bound for the flow rate

To get the limiting value of the flow rate when the fracture aperture goes to zero and the upper bound for the mass flow rate the following simple geometry shown in figure 11 was considered.

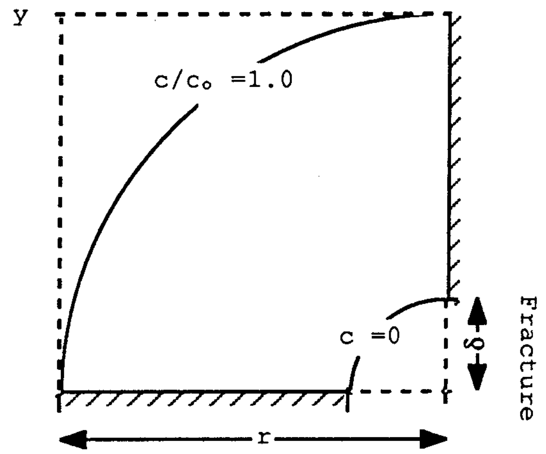

Figure 11 Simplified geometry for the upper bound of flow rate.

In this figure the concentration is kept constant over the outer arc of the circle (at a distance equal to that to the canister) and the concentration at the inner arc (the fracture) remains zero. This condition gives conservative results for cases where the fracture spacing is larger than the thickness of the backfill. This is because the concentration at y=d is less than c_o in reality whereas the approximation says that it is equal to c_o. This means that the simplified case will overestimate the mass flow rates obtained.

The concentration gradient at r = δ is given as (Bird et al, 1960)

$$-\left.\frac{\partial(c/c_0)}{\partial r}\right|_{\delta} = \frac{1}{\delta}\frac{1}{\ln(d/\delta)} \qquad \ldots(24)$$

and the equivalent flow rate at δ is

$$Q_{eq} = \frac{N}{c_0} = D_1 \cdot \frac{\pi \cdot L}{2} \cdot \frac{1}{\ln(\frac{d}{\delta})} \qquad \ldots(25)$$

where $L = 2\pi r_2$ is the length of contact between the rock and the clay.

The solution behavior is also shown in figure 10. The value of the upper bound differs slightly from the actual value when the fracture aperture is large. But as the fracture aperture decreases the values for the upper bound agree well with the actual mass flow rate. Moreover in equation (25), as the aperture decreases the mass flow rate decreases and ultimately reaches zero. This results coincides with the physical situation. This means that if the fracture was sealed and there was no diffusion through the rock, the mass flow rate should be zero.

We can now compare the approximate case of figure 11 with the results for a square area, i.e. a=d. The dimensionless flow rate $\Gamma = \frac{N}{N^0}$, where N^0, as in the case with rectangular geometry, is defined as the nuclide flow rate when there is no resistance to the flow from the surrounding rock.

$$N^0 = D_1 A^0 \frac{\Delta c}{a} \qquad \ldots(26)$$

where $A^0 = d \cdot L$ and since a=d we get $N^0 = D_1 \cdot L \cdot c_0$. The circular case, equation (25) gives N and so

$$\Gamma = \frac{N}{N^0} = \frac{\pi}{2} \frac{1}{\ln\frac{d}{\delta}} \qquad \ldots(27)$$

This is plotted in figure 8.

3.2 DIFFUSION INTO THE ROCK - THE FRACTURE APERTURE IS SEALED COMPLETELY

In this case the fracture aperture is assumed to be sealed completely with impermeable material. Then the nuclides diffuse through the porous rock and eventually arrives at the wall of the fracture where the concentration of nuclides, due to the high water flow rate always is zero.

The governing equation (7) with the boundary conditions (8)-(15) was solved numerically. In this case the value of $7.4 \cdot 10^{-13}$ m^2/s was used for the effective diffusivity of the rock, and $4 \cdot 10^{-11}$ m^2/s was used for the backfill material.

In figure 12 the flux behavior along the fracture wall is shown. The flux at the corner (see figure 4) is higher than in other regions. This means the most mass transport takes place at the corner.

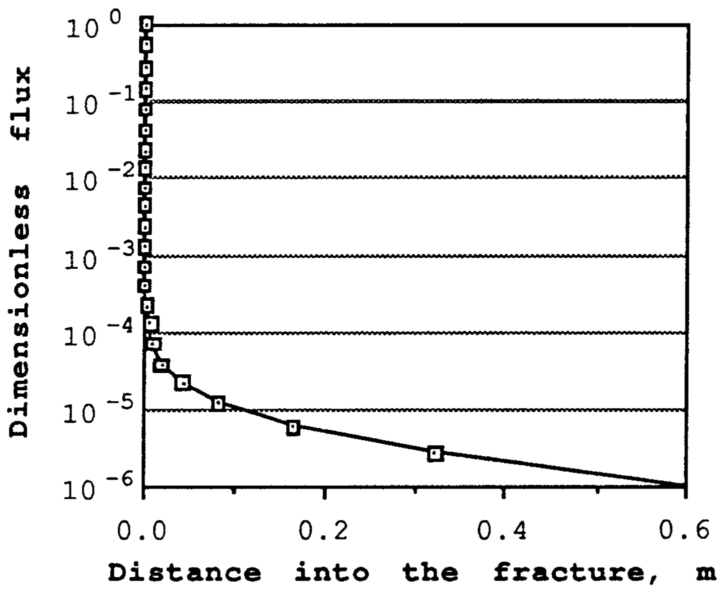

Figure 12 Dimensionless flux into the fracture (fracture aperture=$2 \cdot 10^{-3}$ m, thickness of the backfill =0.38 m, fracture spacing=2 m).

The integral flow rate of nuclides over the fracture wall rate is shown in figure 13.

This figure shows that the first 10 cm of rock carry most of the nuclides(80 %) and that if the fracture could be sealed for some tens of cm the nuclide transport could be strongly decreased.

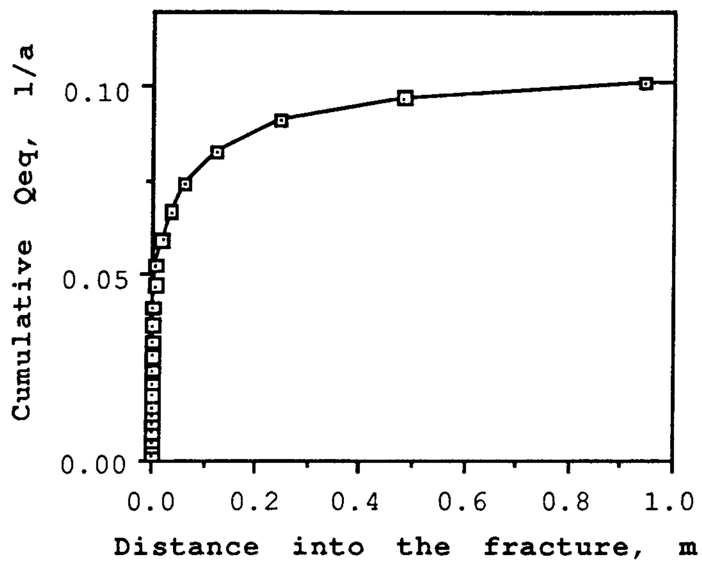

Figure 13 Integral flow rate of nuclides, expressed as Q_{eq} 1/a across the fracture surface (fracture aperture = $2 \cdot 10^{-3}$ m, thickness of the backfill = 0.38 m, fracture spacing = 2 m). Q_{eq} is given per a canister length equal to half a fracture spacing.

3.2.1 Concentration profile assumption at the interface between the rock and backfill material

It is not possible to solve the case with transport through both backfill and rock analytically when the transport goes to the fracture as in the case shown in figure 4 using conventional methods. It would be possible to solve the equations for the backfill region and for the rock region separately provided the concentration profile at the boundary between the regions was known. It is not known, since it would depend on what takes place in the two regions. However, some properties of the concentration profile at the boundary are known and this can be utilized to study the properties of the solution. It would in principle be possible to make a trial solution with the known properties but with some unknown parameter values and

to match the solutions of the two regions by determining the parameter values. This possibility has so far only been explored and may be pursued further at a later stage. The exploratory calculations have however led to some interesting and useful qualitative results.

Figure 14 shows the actual concentration profile along the interface of the rock and the backfill material calculated by the numerical method. It is seen that the concentration rises sharply over a short distance and becomes nearly constant quickly. Although not directly visible in figure 13 or in the numerical results it is known that the concentration profile between the two regions must have the following properties. At x=a for y=d the gradient dc/dy=0. For y=0 at x=a- (just to the left of the boundary) dc/dy=0 also. At x=a+ (just to the right of the boundary) c=0. At the boundary then c=0 and dc/dy=0. For simplicity the fracture aperture which is sealed anyway is taken to be 0. A trial concentration profile can then be constructed so that it has the above properties. The simplest such profile is a step function where c=0 between y=0 and y=β and then suddenly $c=c_o$ for y between β and d, where β is an arbitrarily chosen distance. This is shown in figure 15. An analytical solution for this case is available in the literature (Özisik, 1980). It is given below.

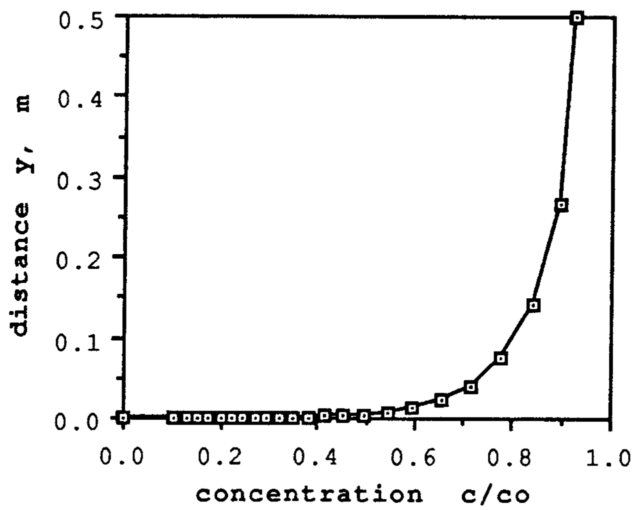

Figure 14 Concentration profile along y direction (fracture aperture=$2 \cdot 10^{-3}$ m, fracture spacing = 2 m, thickness of backfill=0.38 m).

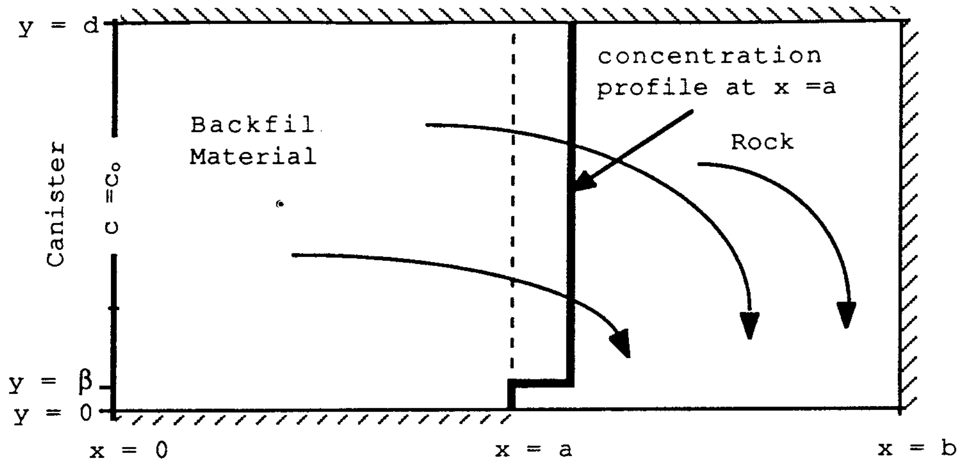

Figure 15 Concentration profile approximation at the interface

$$\frac{c}{c_0} = \sum_{n=1}^{\infty} \frac{2}{d} \frac{1}{\lambda_n} \cos(\lambda_n \beta)\ \sin(\lambda_n y)\ \exp(-\lambda_n (x-a)) \qquad ...(28)$$

where $\lambda_n = n \cdot \pi / 2 \cdot d$ (n = 1,2, ...)

From equation (28), the gradient at the wall of the fracture can be written as

$$\left. \frac{\partial \frac{c}{c_0}}{\partial y} \right|_{y=0} = \sum_{n=1}^{\infty} \frac{2}{d} \cos(\lambda_n \beta)\ \exp(-\lambda_n (x-a)) \qquad ...(29)$$

which can be integrated from x=a to any distance into the rock to obtain the cumulative flow rate. This is illustrated in figure 16.

The flow rate dependency on the distance along the fracture wall for $\beta = 0.001$ m is shown in figure 16. The results are very insensitive to the choice of β as can be seen in figure 17.The results using this approximate method are within a factor of 2 or less compared to those obtained by the numerical method as shown in figure 13, if β is chosen to be between 0.01 and 0.1 m. The method thus can be used to study the qualitative properties of the system.

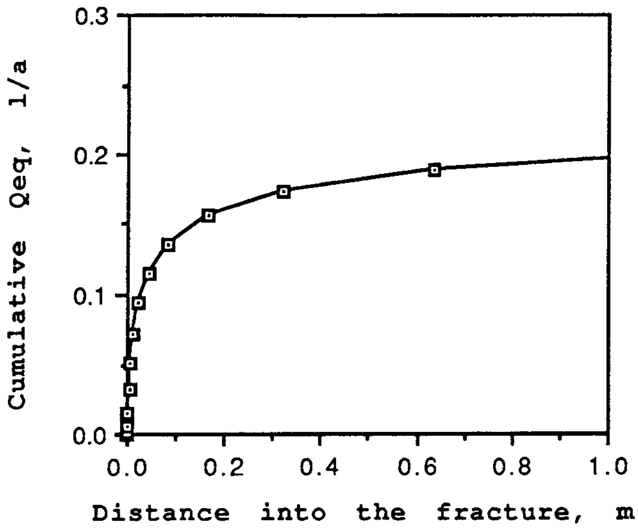

Figure 16 Integral flow rate of nuclides, expressed as Q_{eq} 1/a computed with approximated concentration at the interface backfill/rock (fracture aperture $=2\ 10^{-3}$ m thickness of the backfill = 0.38 m, fracture spacing = 2 m).

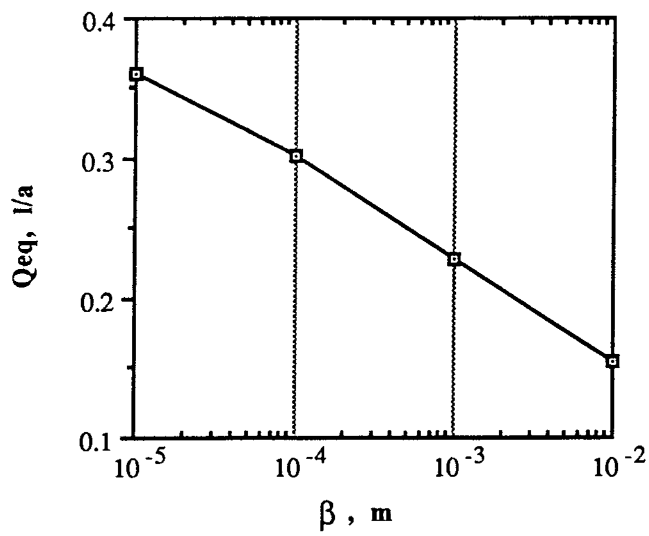

Figure 17 Equivalent flow rate dependency on the arbitrary distance β.

3.3 DIFFUSION AROUND THE EDGE OF THE ROCK

If the concentration at the wall of the rock is assumed to be equal to that at the canister surface, then most of the nuclide flow through the rock will take place near the edge. This case is described by figure 17. In this figure the fracture aperture is assumed to be plugged completely, as well as a portion of the edge of the fracture.

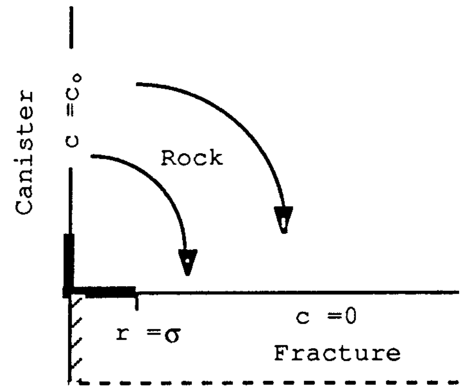

Figure 18 Schematic view of the coating around the edge.

By solving the governing equation (16) with the boundary conditions (17)-(20)(Greenberg,1988), the flux can be obtained as follows.

$$\text{flux} = \frac{D_2}{r}\frac{\partial c}{\partial \theta} = \frac{D_2}{r}\frac{2 \cdot c_0}{\pi} \qquad \ldots(30)$$

Then the nuclide flow rate can be written as

$$Q_{eq} = \frac{N}{c_0} = 2\pi r_2 D_2 \int_{\sigma}^{r} \frac{1}{r}\frac{1}{\pi/2}\, dr = 4 r_2 D_2 \ln\left(\frac{r}{\sigma}\right) \qquad \ldots(31)$$

As shown in equation (31) the flow rate depends strongly on the size of the closed region. As this decreases, the nuclide flow rate increases to infinity. This suggests that if even a small part of the edge is sealed a dramatic reduction of nuclide flow rate can be obtained.

3.4 OVERALL EFFECT OF THE STUDIED DIFFUSION MODELS

An attempt to quantify the total effect of the studied diffusion models would give a picture of the total flow of nuclides into the fracture.

The contributions to the total flow into the fracture is calculated by simply adding the equivalent flows, Q_{eq}, of each diffusion barrier, the backfill, the rock matrix, the backfill material penetrating into the fracture mouth and the film resistance in the fracture itself (Neretnieks, 1986).

We make the assumption here that the pathway through the backfill material from the fracture mouth and the pathway through the rock are independent. This is not strictly true, but is a fair approximation, if either of the pathways has a large resistance compared to the other.

The equivalent flow rate is expressed as the product of a mass transfer koefficient, k_n, a mass transfer area, A_n, and a concentration difference, $\Delta(c/c_0)_n$.

From equation (23) we get for the transport through the clay,

$$Q_{eq}|_b = (kA)_b \cdot \Delta\left(\frac{c}{c_0}\right)_b = \frac{D_1 A \cdot \Delta\left(\frac{c}{c_0}\right)_b}{F(x,y)} \qquad \text{...(32)}$$

from equation (31) we get for the transport through the rock,

$$Q_{eq}|_r = (kA)_r \cdot \Delta\left(\frac{c}{c_0}\right)_r = 4 \cdot D_2 \cdot r_2 \ln\left(\frac{d-\delta}{\sigma}\right) \cdot \Delta\left(\frac{c}{c_0}\right)_r \qquad \text{...(33)}$$

from (Bird et al., 1960) we get for the transport through the clay in the fracture.

$$Q_{eq}|_p = (kA)_p \cdot \Delta\left(\frac{c}{c_0}\right)_p = \frac{D_p \cdot 2\pi\delta}{\ln\left(\frac{r_2+\sigma}{r_2}\right)} \Delta\left(\frac{c}{c_0}\right)_p \qquad \text{...(34)}$$

and from (Neretnieks, 1986) we get the transport in the mobile water,

$$Q_{eq}|_f = (kA)_f \cdot \Delta(\frac{c}{c_0})_f = 2 \cdot (r_2+\sigma) \cdot \delta \sqrt{\frac{4 D_w u_f}{(r_2+\sigma)}} \, \Delta(\frac{c}{c_0})_f \quad \ldots(35)$$

where σ is the distance of penetration into the fracture of the backfill material. D_w is the diffusivity in water and u_f is the velocity of water in the fracture.Dp = $4 \cdot 10^{-10}$ m^2/s is the diffusivity of the clay in the fracture. The indices represent the different diffusion barriers (b - backfill, r - rock matrix, p - backfill penetrated into the fracture mouth and f - diffusion into the water in the fracture). These flow rates are coupled to a total equivalent flow rate $Q_{eq}|_{tot} = k \cdot A_{tot} \Delta(c/c)_{tot}$ as follows.

$\frac{\Delta \frac{c}{c_0}}{Q_{eq}} = \frac{1}{kA}$ is defined as the resistance to the mass transfer

and the total resistance is obtained by adding the local resistances the same way as you calculate the total resistance in an electrical circuit.

In this case the resistances for the rock matrix and the clay filling injected into the fracture are coupled in parallell, consequently the total resistance will be

$$(\frac{1}{kA})_{tot} = (\frac{1}{kA})_b + (\frac{1}{(kA)_r + (kA)_p}) + (\frac{1}{kA})_f \quad \ldots(36)$$

At this stage it is not possible to calculate this function, since in this report the separate diffusion barriers have been calculated with different assumptions and boundary conditions. However, by plotting (see figure 19) the equivalent flow rates for each of the calculated cases against the water flow in the fracture, with fracture width (δ) and penetration depth (σ) as parameters, we can see in which intervals of water flow the different resistance will be dominant. For high water fluxes u_0 in the rock the diffusion resistance in the backfill in the

hole will start to play a role. For lower water fluxes the resistance in the mobile water dominates. If the fracture can be sealed over a few tens of centimeters the nuclide flux will be strongly limited. For example for s = 0.2 m Qeq is reduced to less than 0.04 l/a for one meter of canister.

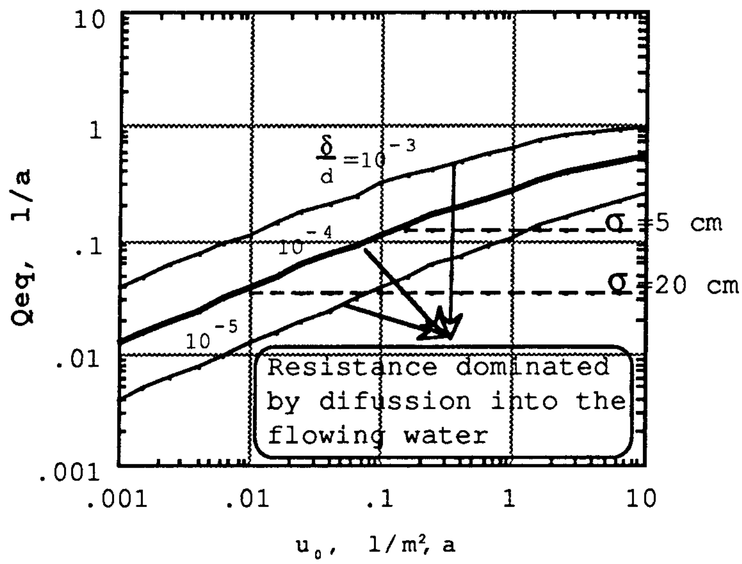

Figure 19 Resistance to nuclide migration into the fracture represented as equivalent nuclide flow in the different diffusion barriers. The pathway through the rock is not included in the figure.

4 CONCLUSION

Two different cases were studied to analyze the influence of the fracture aperture on the mass flow rate. In addition the extreme case for the penetration of nuclide at the aperture edge was also studied. In summary the following was found.

For diffusion into the fracture aperture with impermeable rock it was found that for very high flow rates of water in the fracture, so high that the concentration is maintained at c=0, the nuclide flow rate monotonically increases with the fracture aperture. The order of magnitude of Q_{eq} is 1 l/a and meter of canister using an effective diffusivity for the backfill of $4 \cdot 10^{-11}$ m^2/s. Only the resistance in the backfill is then accounted for.

For diffusion through the rock only (the fracture aperture is plugged) it was found that for an effective diffusivity of $7.4 \cdot 10^{-13}$ m^2/s for the rock the equivalent nuclide flow rate, Q_{eq} is in the order of 0.1 l/a per meter of canister, much less than what can be going through the fracture mouth.

The equivalent flow rate increases steeply with decreasing sealed distance around the apex. This indicates that even a limited filling of the fracture aperture reduces the nuclide flow rate remarkably. This applies both for the pathway through the rock and through the sealed fracture portion to the water.

In summary the transport of nuclides through the rock to the flowing water is small compared to that directly through the mouth of the fracture even for very high water flow rates. If the fracture can be sealed some 10's of centimeters the flow rate decreases dramatically.

NOTATION

a	:	backfill thickness (m)
A	:	area (m^2)
b	:	assumed distance as infinity in x direction (m)
c	:	concentration ($mole/m^3$)
c_o	:	concentration at the canister wall ($mole/m^3$)
d	:	a half distance between fractures (m)
D_1	:	effective diffusivity in backfill (m^2/s)
D_2	:	effective diffusivity in rock (m^2/s)
D_p	:	effective diffusivity in clay in the fracture (m^2/s)
D_w	:	effective diffusivity in the mobile water (m^2/s)
$F(x,y)$	:	summation term in equation (21)
n		summation constant in equation (21)
N	:	mass flow rate (mole/s)
N^0		reference flow rate (mole/s)
Q_{eq}		equivalent flow rate, N/c_0 (l/a)
r	:	radial coordinate (m)
r_1		radius of canister (m)
r_2		radius of canister + backfill (m)
u_f		velocity of water in the fracture (m/a)
u_0		water flux in the bed rock ($l/m^2,a$)
x	:	distance into the fracture (m)
y	:	distance to longitudinal canister axis (m)

Greek letter

β		arbitrary distance (m)
δ	:	a half of fracture aperture (m)
ε	:	error bound in equation (26)
λ_n	:	eigenvalue in equation (26) (m^{-1})
θ	:	angular coordinate (radians)
Γ		dimensionless flow rate, N/N^o
σ		depth of backfill penetration into fracture (m)

REFERENCES

Anderson, G., A Rasmuson, and I. Neretnieks, "Migration Model for the Near Field: Final Report", KBS TR 82-24 1982

Bird, R.B., Stewart, W.E. and Lightfoot, E.N., Transport Phenomena, Wiley & Sons 1960 p 548

Carslaw, H. S. and J. C. Jaeger, Conduction of Heat in Solids, 2nd ed., Oxford Univ. Press 1959

Greenberg, M. D., Advanced Engineering Mathematics, Prentice-Hall Inc. 1988.

KBS-3, "Final Storage of Spent Nuclear Fuel", Swedish Nuclear Fuel Supply Co., Division KBS May 1983.

Lapidus, L. and G. F. Pinder, Numerical Solution of Partial Differential Equations in Science and Engineering, John Wiley & Sons 1982

Neretnieks, I., "Retardation of Escaping Nuclides from a Final Repository", KBS Teknisk Rapport, No. 30 1977

Neretnieks, I., "Transport of Oxidants and Radionuclides through a Clay Barrier", KBS TR 79 1978

Neretnieks, I., "Stationary Transport of Dissolved Species in the Backfill Surrounding a Waste Canister in Fissured Rock: Some Simple Analytical Solutions", Nuclear Technology, 72, 194 1986

Rasmuson, A., Narasimhan, T.N. and Neretnieks, I., "Chemical Transport in a fissured rock. Verification of a numerical model", Water Resources Res. 18, pp 1479-1492, 1982

Özisik, N.M., Heat Conduction, Wiley & Sons 1980, p 64-65

List of SKB reports

Annual Reports

1977–78
TR 121
KBS Technical Reports 1 – 120.
Summaries. Stockholm, May 1979.

1979
TR 79–28
The KBS Annual Report 1979.
KBS Technical Reports 79-01 – 79-27.
Summaries. Stockholm, March 1980.

1980
TR 80–26
The KBS Annual Report 1980.
KBS Technical Reports 80-01 – 80-25.
Summaries. Stockholm, March 1981.

1981
TR 81–17
The KBS Annual Report 1981.
KBS Technical Reports 81-01 – 81-16.
Summaries. Stockholm, April 1982.

1982
TR 82–28
The KBS Annual Report 1982.
KBS Technical Reports 82-01 – 82-27.
Summaries. Stockholm, July 1983.

1983
TR 83–77
The KBS Annual Report 1983.
KBS Technical Reports 83-01 – 83-76
Summaries. Stockholm, June 1984.

1984
TR 85–01
Annual Research and Development Report 1984
Including Summaries of Technical Reports Issued during 1984. (Technical Reports 84-01 – 84-19)
Stockholm June 1985.

1985
TR 85-20
Annual Research and Development Report 1985
Including Summaries of Technical Reports Issued during 1985. (Technical Reports 85-01-85-19)
Stockholm May 1986.

1986
TR 86-31
SKB Annual Report 1986
Including Summaries of Technical Reports Issued during 1986
Stockholm, May 1987

1987
TR 87-33
SKB Annual Report 1987
Including Summaries of Technical Reports Issued during 1987
Stockholm, May 1988

1988
TR 88-32
SKB Annual Report 1988
Including Summaries of Technical Reports Issued during 1988
Stockholm, May 1989

Technical Reports

1989

TR 89-01
Near-distance seismological monitoring of the Lansjärv neotectonic fault region Part II: 1988
Rutger Wahlström, Sven-Olof Linder, Conny Holmqvist, Hans-Edy Mårtensson
Seismological Department, Uppsala University, Uppsala
January 1989

TR 89-02
Description of background data in SKB database GEOTAB
Ebbe Eriksson, Stefan Sehlstedt
SGAB, Luleå
February 1989

TR 89-03
Characterization of the morphology, basement rock and tectonics in Sweden
Kennert Röshoff
August 1988

TR 89-04
SKB WP-Cave Project
Radionuclide release from the near-field in a WP-Cave repository
Maria Lindgren, Kristina Skagius
Kemakta Consultants Co, Stockholm
April 1989

TR 89-05
SKB WP-Cave Project
Transport of escaping radionuclides from the WP-Cave repository to the biosphere
Luis Moreno, Sue Arve, Ivars Neretnieks
Royal Institute of Technology, Stockholm
April 1989

TR 89-06
SKB WP-Cave Project
Individual radiation doses from nuclides contained in a WP-Cave repository for spent fuel
Sture Nordlinder, Ulla Bergström
Studsvik Nuclear, Studsvik
April 1989

TR 89-07
SKB WP-Cave Project
Some Notes on Technical Issues
Part 1: Temperature distribution in WP-Cave: when shafts are filled with sand/water mixtures
Stefan Björklund, Lennart Josefson
Division of Solid Mechanics, Chalmers University of Technology, Gothenburg, Sweden
Part 2: Gas and water transport from WP-Cave repository Luis Moreno, Ivars Neretnieks
Department of Chemical Engineering, Royal Institute of Technology, Stockholm, Sweden
Part 3: Transport of escaping nuclides from the WP-Cave repository to the biosphere. Influence of the hydraulic cage
Luis Moreno, Ivars Neretnieks
Department of Chemical Engineering, Royal Institute of Technology, Stockholm, Sweden
August 1989

TR 89-08
SKB WP-Cave Project
Thermally incuded convective motion in groundwater in the near field of the WP-Cave after filling and closure
Polydynamics Limited, Zürich
April 1989

TR 89-09
An evaluation of tracer tests performed at Studsvik
Luis Moreno[1], Ivars Neretnieks[1], Ove Landström[2]
[1] The Royal Institute of Technology, Department of Chemical Engineering, Stockholm
[2] Studsvik Nuclear, Nyköping
March 1989

TR 89-10
Copper produced from powder by HIP to encapsulate nuclear fuel elements
Lars B Ekbom, Sven Bogegård
Swedish National Defence Research Establishment
Materials department, Stockholm
February 1989

TR 89-11
Prediction of hydraulic conductivity and conductive fracture frequency by multivariate analysis of data from the Klipperås study site
Jan-Erik Andersson[1], Lennart Lindqvist[2]
[1] Swedish Geological Co, Uppsala
[2] EMX-system AB, Luleå
February 1988

TR 89-12
Hydraulic interference tests and tracer tests within the Brändan area, Finnsjön study site
The Fracture Zone Project – Phase 3
Jan-Erik Andersson, Lennart Ekman, Erik Gustafsson, Rune Nordqvist, Sven Tirén
Swedish Geological Co, Division of Engineering Geology
June 1988

TR 89-13
Spent fuel
Dissolution and oxidation
An evaluation of literature data
Bernd Grambow
Hanh-Meitner-Institut, Berlin
March 1989

TR 89-14
The SKB spent fuel corrosion program
Status report 1988
Lars O Werme[1], Roy S Forsyth[2]
[1] SKB, Stockholm
[2] Studsvik AB, Nyköping
May 1989

TR 89-15
Comparison between radar data and geophysical, geological and hydrological borehole parameters by multivariate analysis of data
Serje Carlsten, Lennart Lindqvist, Olle Olsson
Swedish Geological Company, Uppsala
March 1989

TR 89-16
Swedish Hard Rock Laboratory – Evaluation of 1988 year pre-investigations and description of the target area, the island of Äspö
Gunnar Gustafsson, Roy Stanfors, Peter Wikberg
June 1989

TR 89-17
Field instrumentation for hydrofracturing stress measurements
Documentation of the 1000 m hydrofracturing unit at Luleå University of Technology
Bjarni Bjarnason, Arne Torikka
August 1989

TR 89-18
Radar investigations at the Saltsjötunnel – predicitions and validation
Olle Olsson[1] and Kai Palmqvist[2]
[1] Abem AB, Uppsala, Sweden
[2] Bergab, Göteborg
June 1989

TR 89-19
Characterization of fracture zone 2, Finnsjön study-site
Editors: K. Ahlbom, J.A.T. Smellie, Swedish Geological Co, Uppsala
Part 1: Overview of the fracture zone project at Finnsjön, Sweden
K. Ahlbom and J.A.T. Smellie. Swedish Geological Company, Uppsala, Sweden.
Part 2: Geological setting and deformation history of a low angle fracture zone at Finnsjön, Sweden
Sven A. Tirén. Swedish Geological Company, Uppsala, Sweden.
Part 3: Hydraulic testing and modelling of a low-angle fracture zone at Finnsjön, Sweden
J-E. Andersson[1], L. Ekman[1], R. Nordqvist[1] and A. Winberg[2]
[1] Swedish Geological Company, Uppsala, Sweden
[2] Swedish Geological Company, Göteborg, Sweden
Part 4: Groundwater flow conditions in a low angle fracture zone at Finnsjön, Sweden
E. Gustafsson and P. Andersson. Swedish Geological Company, Uppsala, Sweden
Part 5: Hydrochemical investigations at Finnsjön, Sweden
J.A.T. Smellie[1] and P. Wikberg[2]
[1] Swedish Geological Company, Uppsala, Sweden
[2] Swedish Nuclear Fuel and Waste Management Company, Stockholm, Sweden
Part 6: Effects of gas-lift pumping on hydraulic borehole conditions at Finnsjön, Sweden
J-E- Andersson, P. Andersson and E. Gustafsson. Swedish Geological Company, Uppsala, Sweden
August 1989

TR 89-20
WP-Cave - Assessment of feasibility, safety and development potential
Swedish Nuclear Fuel and Waste Management Company, Stockholm, Sweden
September 1989

TR 89-21
Rock quality designation of the hydraulic properties in the near field of a final repository for spent nuclear fuel
Hans Carlsson[1], Leif Carlsson[1], Roland Pusch[2]
[1] Swedish Geological Co, SGAB, Gothenburg, Sweden
[2] Clay Technology AB, Lund, Sweden
June 1989

TR 89-22
Diffusion of Am, Pu, U, Np, Cs, I and Tc in compacted sand-bentonite mixture
Department of Nuclear Chemistry, Chalmers University of Technology, Gothenburg, Sweden
August 1989

TR 89-23
Deep ground water microbiology in Swedish granitic rock and it's relevance for radionuclide migration from a Swedish high level nuclear waste repository
Karsten Pedersen
University of Göteborg, Department of Marine microbiology, Gothenburg, Sweden
March 1989

TR 89-24
Some notes on diffusion of radionuclides through compacted clays
Trygve E Eriksen
Royal Institute of Technology, Department of Nuclear Chemistry, Stockholm, Sweden
May 1989

TR 89-25
Radionuclide sorption on crushed and intact granitic rock
Volume and surface effects
Trygve E Eriksen, Birgitta Locklund
Royal Institute of Technology, Department of Nuclear Chemistry, Stockholm, Sweden
May 1989

TR 89-26
Performance and safety analysis of WP-Cave concept
Kristina Skagius[1], Christer Svemar[2]
[1] Kemakta Konsult AB
[2] Swedish Nuclear Fuel and Waste Management Co
August 1989

TR-89-27
Post-excavation analysis of a revised hydraulic model of the Room 209 fracture, URL, Manitoba, Canada
A part of the joint AECL/SKB characterization of the 240 m level at the URL, Manitoba, Canada
Anders Winberg[1], Tin Chan[2], Peter Griffiths[2], Blair Nakka[2]
[1] Swedish Geological Co, Gothenburg, Sweden
[2] Computations & Analysis Section, Applied Geoscience Branch, Atomic Energy of Canada Limited, Pinawa, Manitoba, Canada
October 1989

TR 89-28
Earthquake mechanisms in Northern Sweden Oct 1987 — Apr 1988
Ragnar Slunga
October 1989

TR 89-29
Interim report on the settlement test in Stripa
Lennart Börgesson, Roland Pusch
Clay Technology AB, Lund
November 1989

TR 89-30
Seismic effects on bedrock and underground constructions. A literature survey of damage on constructions, changes in groundwater levels and flow, changes in chemistry in groundwater and gases
Kennert Röshoff
June 1989

TR 89-31
Interdisciplinary study of post-glacial faulting in the Lansjärv area Northern Sweden 1986–1988
Göran Bäckblom, Roy Stanfors (eds.)
December 1989

TR-89-32
Influence of various excavation techniques on the structure and physical properties of "near-field" rock around large boreholes
Roland Pusch
Clay Technology AB and Lund University of Technology and Natural Sciences, Lund
December 1989

TR 89-33
Investigation of flow distribution in a fracture zone at the Stripa mine, using the radar method, results and interpretation
Per Andersson, Peter Andersson, Erik Gustafsson, Olle Olsson
Swedish Geological Co., Uppsala, Sweden
December 1989

TR 89-34
Transport and microstructural phenomena in bentonite clay with respect to the behavior and influence of Na, Cu and U
Roland Pusch[1], Ola Karnland[1], Arto Muurinen[2]
[1] Clay Technology AB (CT)
[2] Technical Research Center of Finland, Reactor Laboratory (VTT)
December 1989

TR 89-35
The joint SKI/SKB scenario development project
Editor: Johan Andersson[1]
Authors: Johan Andersson[1], Torbjörn Carlsson[1], Torsten Eng[2], Fritz Kautsky[1], Erik Söderman[3], Stig Wingefors[1]
[1] Statens Kärnkraftsinspektion, SKI Stockholm, Sweden
[2] Svensk Kärnbränslehantering AB, SKB, Stockholm, Sweden
[3] ES-Konsult, Bromma, Sweden
December 1989

TR-89-36
^{14}C-Analyses of calcite coatings in open fractures from the Klipperås study site, Southern Sweden
Götan Possnert[1], Eva-Lena Tullborg[2]
[1] Svedberg-laboratoriet, Uppsala
[2] Sveriges Geologiska AB, Gothenburg
November 1989

TR 89-37
Alteration of natural UO_2 under oxidizing conditions from Shinkolobwe, Katanga, Zaire:
A natural analogue for the corrosion of spent fuel
R J Finch, R C Ewing
Department of Geology, University of New Mexico
November 1989